



**University of
Zurich**^{UZH}

**Zurich Open Repository and
Archive**

University of Zurich
University Library
Strickhofstrasse 39
CH-8057 Zurich
www.zora.uzh.ch

Year: 2016

Variable phenotype and discrete alterations of immune phenotypes in CTP synthase 1 deficiency: Report of 2 siblings

Trück, Johannes ; Kelly, Dominic F ; Taylor, John M ; Kienzler, Anne Kathrin ; Lester, Tracy ; Seller, Anneke ; Pollard, Andrew J ; Patel, Smita Y

DOI: <https://doi.org/10.1016/j.jaci.2016.04.059>

Posted at the Zurich Open Repository and Archive, University of Zurich

ZORA URL: <https://doi.org/10.5167/uzh-126132>

Journal Article

Accepted Version



The following work is licensed under a Creative Commons: Attribution-NonCommercial-NoDerivatives 4.0 International (CC BY-NC-ND 4.0) License.

Originally published at:

Trück, Johannes; Kelly, Dominic F; Taylor, John M; Kienzler, Anne Kathrin; Lester, Tracy; Seller, Anneke; Pollard, Andrew J; Patel, Smita Y (2016). Variable phenotype and discrete alterations of immune phenotypes in CTP synthase 1 deficiency: Report of 2 siblings. *Journal of Allergy and Clinical Immunology*, 138(6):1722-1725.e6.

DOI: <https://doi.org/10.1016/j.jaci.2016.04.059>

Letter to the Editor

Variable phenotype and discrete alterations of immune phenotypes in CTP synthase 1 deficiency: Report of 2 siblings

To the Editor:

Loss-of-function homozygous mutations in the CTP synthase 1 (*CTPS1*) gene in humans have only recently been discovered and reveal the role of this gene in lymphocyte proliferation.¹ To date a single report including 8 individuals describes a severe clinical phenotype including early onset of severe chronic viral infections, recurrent encapsulated bacterial infections, and EBV-related B-cell non-Hodgkin lymphoma.¹

We report 2 further sibling cases of *CTPS1* deficiency identified through whole-exome sequencing (WES), further illustrating the phenotype of *CTPS1* deficiency and demonstrating the value of WES for rapid diagnosis of primary immunodeficiency even for conditions whose phenotype is not well recognized.

The 2 siblings (boy, now 6 years old; girl, now 3 years old) described in this report are the only children of nonconsanguineous and healthy white parents with no personal or family history of immunodeficiency, autoimmunity, or EBV-related disorders. Both children had no dysmorphic features and normal growth.

The boy was born at term and was noted to have a significant burden of infections from early infancy. He was admitted to hospital at age 2 months with fever, lethargy, and poor feeding of unknown cause, responding rapidly to 48 hours of intravenous antibiotics. At age 7 months, he had an episode of invasive serotype 19A pneumococcal disease despite prior vaccination with the 13-valent pneumococcal conjugate vaccine (Prev(e)nar 13, Pfizer Inc, New York, NY) at age 2 and 4 months. At age 16 months, while on holiday in Turkey, he was admitted to hospital with severe tonsillitis and dehydration. At the age of 34 months, he developed an acute EBV infection with persistent viremia (see Fig E1 in this article's Online Repository at www.jacionline.org) but no features of hemophagocytic lymphohistiocytosis.

In addition to these hospital admissions, he suffered from recurrent otitis media and lower respiratory tract infections, and had moderate to severe eczema from the neonatal period. He developed chronic diarrhea of unknown etiology lasting for approximately 8 weeks when he was 3.5 years old. An upper and lower gastrointestinal endoscopic biopsy showed reactive lymphoid aggregates in the duodenum and colon without signs of active inflammation, ulceration, or infectious organisms.

The immunologic workup was largely normal (see Table E1 and the Methods section in this article's Online Repository at www.jacionline.org). However, he had only moderate responses to a 13-valent pneumococcal conjugate vaccine booster with poor persistence² of vaccine antibodies (Fig 1). He also showed rapid waning of antibodies against *H influenzae* type b polysaccharide and tetanus toxoid protein.

His younger sister first presented at the age of 8 months with a likely viral illness involving fever, possible meningitis (mild pleocytosis) and unresponsive episodes along with vomiting, and prolonged diarrhea. She also suffered from eczema and recurrent

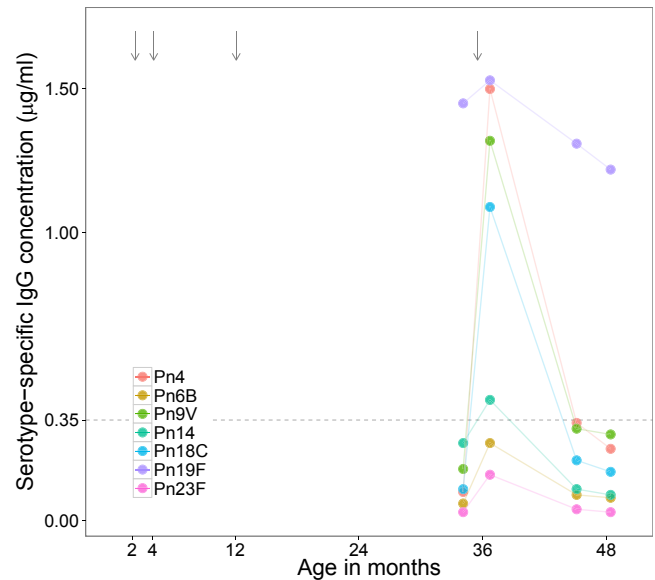


FIG 1. Pneumococcal serotype-specific antibody concentrations before and after booster vaccination at age 35 months. Pn, Pneumococcal serotype. Arrows indicate age at vaccination with the 13-valent pneumococcal conjugate vaccine (Prev(e)nar 13, Pfizer Inc); the dashed line specifies a serotype-specific IgG concentration of 0.35 µg/mL.

upper and lower respiratory tract infections from age 12 months. However, she did not have frequent ear infections, had never suffered from invasive bacterial diseases, and remains EBV negative by both PCR and serology. Initial immunological testing was normal (Table E1) apart from a poor response to a booster dose of pneumococcal conjugate vaccine and undetectable anti-*H influenzae* type b IgG concentration despite booster vaccination.

Detailed analysis of cytokine production in both children showed a normal T_H1 axis and normal TLR responses. However, IFN- γ production in response to T-cell agonists was significantly reduced, pointing to T-cell impairment (see Fig E2 in this article's Online Repository at www.jacionline.org).

Following negative results upon initial investigation for causes of immunodeficiency, targeted WES was performed on the affected boy when he was 4 years old. A homozygous variant within the final nucleotide in intron 17 of the *CTPS1* gene (NM_001905.2:c.1692-1G>C) was thought to be causative (see the Methods section).

Flow cytometric analysis of lymphocytes at the age of 59 and 25 months, respectively, revealed lymphopenia and marked deficiency of B cells in the boy (Fig 2, A and B), possibly resulting from chronic EBV infection (Fig E1). Both children showed a relative predominance of transitional B cells and a deficiency of naive B cells (Fig 2, C). The distribution of major T cells (Fig 2, D) and $CD4^+$ T-cell subpopulations was largely unaffected (Fig 2, E), whereas major disturbances were seen within the $CD8^+$ T-cell compartment (Fig 2, F).

The identification of the *CTPS1* mutation has significantly altered the clinical management of the 2 affected siblings, emphasizing the clinical use of next-generation sequencing in children with unknown immunodeficiencies. The index case has already

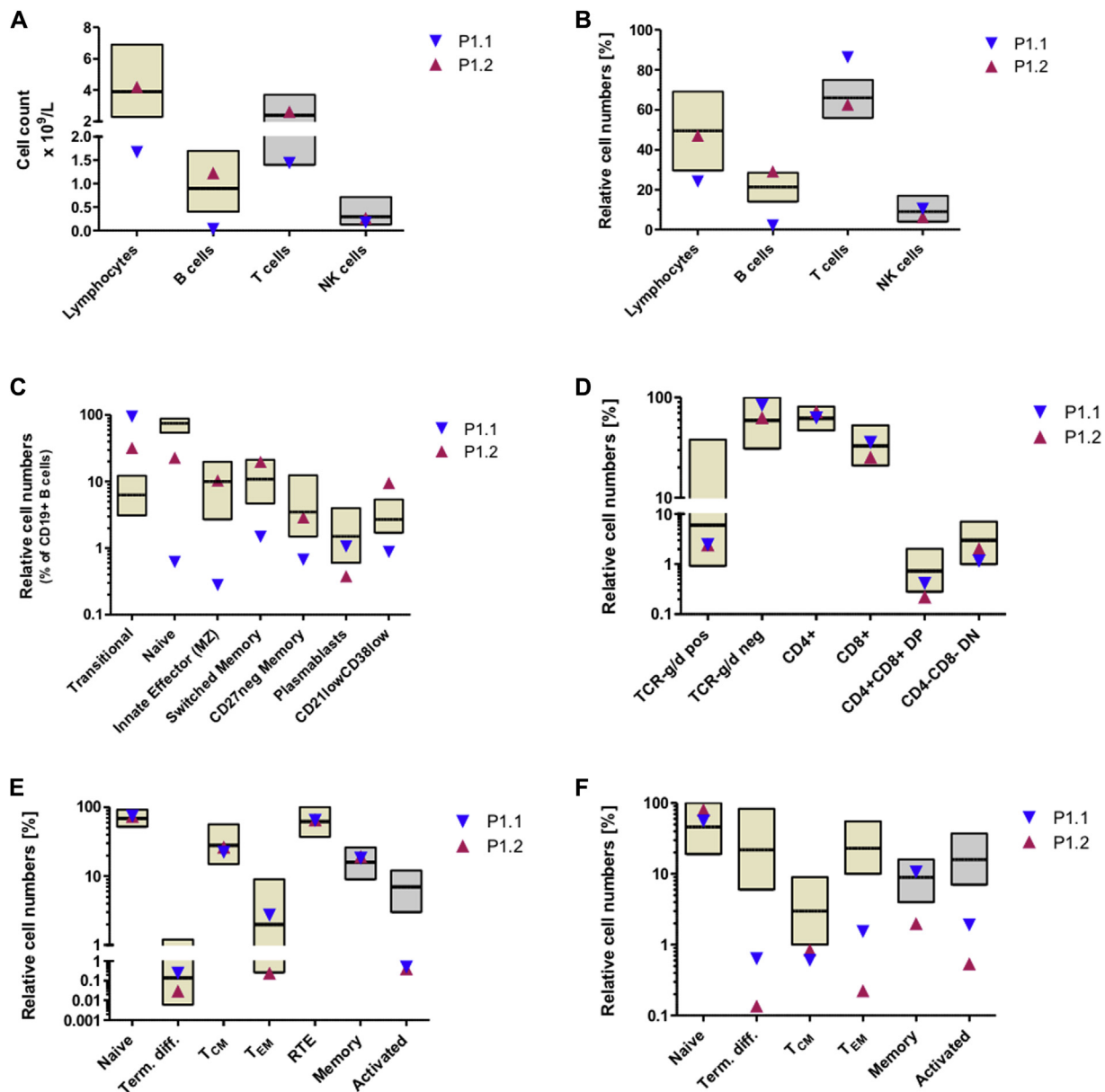


FIG 2. A, Absolute lymphocyte and B-, T-, and NK-cell counts. B, Relative lymphocyte and B-, T-, and NK-cell values. C, Relative numbers for B-cell subpopulations. D, Relative frequencies of major T-cell subsets. E, Relative frequencies of CD4⁺ T-cell subpopulations. F, Relative frequencies of CD8⁺ T-cell subpopulations. DN, Double negative; DP, double positive; NK, natural killer; T_{CM}, central memory T cells; T_{EM}, effector memory T cells; RTE, recent thymic emigrants.

successfully undergone matched unrelated donor hematopoietic stem cell transplantation (HSCT) using peripheral blood stem cells following reduced intensity conditioning with fludarabine and melphalan and *in vivo* T-cell depletion with alemtuzumab. He is now 8 months after HSCT at home and doing well without signs of graft-versus-host disease. The sister is on immunoglobulin replacement therapy and being considered for HSCT.

This report adds to the current literature by highlighting that CTPS1 deficiency can also manifest with relatively mild clinical phenotype as seen in the sister of the index case. We suggest that CTPS1 deficiency should be considered in all patients with a phenotype of combined immunodeficiency and without alternative diagnosis.³ An important feature of CTPS1-deficient patients

is that they may present with only subtle laboratory abnormalities of the humoral immune system despite experiencing severe bacterial disease. In addition, CTPS1-deficient patients can have normal immunophenotypes of major T-cell populations (Fig 2, D) and normal T-cell proliferation to mitogens. We found increased frequencies of transitional B cells in combination with reduced frequencies of naive B cells in both children (Fig 2, C). In the index patient, frequencies of naive, marginal zone, and memory B cells were greatly reduced (Fig 2, C), likely as a result of poor EBV control. Reduced numbers of memory B cells were also found in several patients in the original report¹ but here we show that this finding may not represent an inherent feature of CTPS1 deficiency and rather a result of chronic EBV infection.

Hence, memory B-cell frequencies may be normal in CTPS1-deficient patients before EBV exposure. Within the T-cell compartment, we found reduced frequencies of activated CD4⁺ and CD8⁺ T cells in both patients whereas other CD4⁺ T-cell subpopulations were present at normal frequencies. These findings are in line with results in 4 of the 8 patients described in the original report¹ who did not show lymphopenia or reduced numbers of naive CD4⁺ T cells and therefore these recently suggested diagnostic features⁴ may not be sensitive in identifying CTPS1-deficient patients. We found marked alterations of the CD8⁺ T-cell compartment in our patients, mainly reduced frequencies of terminally differentiated and memory CD8⁺ subpopulations (Fig 2, F), possibly as a result of both chronic EBV infection and the underlying defect in *CTPS1*. Taken together, CTPS1 deficiency may be suggested in children with recurrent viral and bacterial infections and reduced frequencies of activated CD4/8⁺ T cells and abnormal CD8⁺ phenotype with a predominance of naive CD8⁺ T cells. Abnormalities of lymphocyte numbers, naive CD4⁺ T-cell, and memory B-cell frequencies and the capacity of T cells to proliferate upon exposure to mitogens seem to be variable features and may also depend on previous exposure to EBV.

CTPS1 deficiency expands the range of primary immune deficiencies associated with poor EBV control and lymphoproliferation.³ At present very little is known about the clinical phenotype or prognosis of patients with CTPS1 deficiency. Our 2 patients presented with clinical features suggestive of combined immunodeficiency and in contrast to previously described cases,¹ the clinical features also included gastrointestinal symptoms and eczema, possibly as a result of immune dysregulation. These latter features have not previously been described in CTPS1-deficient patients.

The utility of next-generation DNA sequencing in the diagnosis of rare diseases is now widely appreciated.⁵ This technology offers rapid and cost-effective detection of known mutations in *PID* genes. In this report, we demonstrate that in a clinical setting where a range of genotypes may be responsible for the observed phenotype, WES offers a novel approach in establishing a definitive diagnosis affecting the proband and other family members.

We thank the High-Throughput Genomics Group at the Wellcome Trust Centre for Human Genetics (funded by Wellcome Trust grant reference no. 090532/Z/09/Z and Medical Research Council Hub grant no. G0900747 91070) for the generation of the sequencing data.

Johannes Trück, MD, DPhil^a

Dominic F. Kelly, MRCP, PhD^a

John M. Taylor, PhD^b

Anne Kathrin Kienzler, PhD^c

Tracy Lester, FRCPATH, PhD^b

Anne Seller, FRCPATH, PhD^b

Andrew J. Pollard, FRCPCH, PhD^a

Smita Y. Patel, FRCP, FRCPATH, PhD^c

From ^athe Department of Paediatrics, University of Oxford, and the NIHR Oxford Biomedical Research Centre, Oxford, United Kingdom; ^bOxford Medical Genetics Laboratories, Oxford University Hospitals NHS Trust, The Churchill Hospital, Headington, Oxford, United Kingdom; and ^cthe Clinical Immunology Group, Oxford NIHR Biomedical Research Centre, United Kingdom. E-mail: johannes.truck@kispi.uzh.ch.

This work was supported by the National Institute for Health Research (NIHR) Biomedical Research Centre Oxford with funding from the Department of Health's NIHR Biomedical Research Centres funding scheme.

Disclosure of potential conflict of interest: D. F. Kelly has received grants from the Biotechnology and Biological Sciences Research Council and GlaxoSmithKline and has received travel support from GlaxoSmithKline and Sanofi-Pasteur. S. Y. Patel has received grants from the Wellcome Trust and has received payment for lectures from Biotest and Activis. The rest of the authors declare that they have no relevant conflicts of interest.

REFERENCES

1. Martin E, Palmic N, Sanquer S, Lenoir C, Hauck F, Mongellaz C, et al. CTP synthase 1 deficiency in humans reveals its central role in lymphocyte proliferation. *Nature* 2014;510:288-92.
2. Trück J, Snape MD, Tatangeli F, Voysey M, Yu LM, Faust SN, et al. Pneumococcal serotype-specific antibodies persist through early childhood after infant immunization: Follow-up from a randomized controlled trial. *PLoS One* 2014;9:e91413.
3. Taylor GS, Long HM, Brooks JM, Rickinson AB, Hislop AD. The immunology of Epstein-Barr virus-induced disease. *Annu Rev Immunol* 2015;33:787-821.
4. Bonilla FA, Khan DA, Ballas ZK, Chinen J, Frank MM, Hsu JT, et al. Practice parameter for the diagnosis and management of primary immunodeficiency. *J Allergy Clin Immunol* 2015;136:1186-205, e1-78.
5. Casanova J-L, Conley ME, Seligman SJ, Abel L, Notarangelo LD. Guidelines for genetic studies in single patients: lessons from primary immunodeficiencies. *J Exp Med* 2014;211:2137-49.

<http://dx.doi.org/10.1016/j.jaci.2016.04.059>

METHODS

Additional immune workup in the index case

In addition to the analysis presented in Table E1, normal results were found for T-cell receptor V-beta repertoire, T-cell-receptor gene rearrangement excisional circles, CD62 ligand shedding, SLAM-associated protein and X-linked inhibitor of apoptosis protein expression, and IL-2-inducible T-cell kinase expression and genetic analysis.

Whole-exome sequencing

This was done as part of a research project approved by the Southampton A Research Ethics Committee (reference 12/SC/044), and written informed consent was obtained from both parents.

Exome capture was performed using the NimbleGen SeqCap EZ Human Exome Library v2.0, according to the manufacturer's instructions, and sequenced using a 2×100 bp read protocol on an Illumina HiSeq. Approximately 15 Gb of sequence was obtained, providing at least $10 \times$ vertical read depth over approximately 90% of the coding exome, as specified by the consensus coding sequence project. Reads were aligned to hg19 with Stampy (v1.0.20)^{E1} and variant calling of single nucleotide variants and short insertion and deletions was undertaken using Platypus (v0.5.2; www.well.ox.ac.uk/platypus).^{E2}

Variant annotation and analysis was restricted to a targeted panel of 237 immune-related genes (Table E2), using the Illumina VariantStudio data analysis software (Illumina, Inc, San Diego, Calif). Variants were initially filtered on a population frequency below 5% within the National Heart, Lung, and Blood Institute GO Exome Sequencing Project,^{E3} which reduced the list from 284 variants to 44 variant calls. All variants were individually assessed to determine their likely pathogenicity on the basis of ACGS-recommended best practice guidelines.^{E4}

Subsequent Sanger sequencing demonstrated that this homozygous nucleotide substitution was present in both affected children and heterozygous in both unaffected parents. This change has recently been described in several affected members of families originating from the northwest of England^{E5} and disrupts 1 of the 2 invariant nucleotides of the acceptor site and is predicted to lead to aberrant splicing of intron 17 (Alamut, version 2.4.5; Interactive Bio-software, Rouen, France) (Fig E3). It is therefore considered to be pathogenic.

Immune phenotyping by flow cytometry

Absolute lymphocyte counts were determined using the BD Multitest, CD3/CD16:56/CD45/CD19 reagent, and TruCount tubes (both BD Biosciences, San Jose, Calif) according to the manufacturer's instructions. Flow cytometry data were analyzed with Infinicyt software (Cytognos, Spain). Boxplots indicate the 5 to 95th percentile and median adopted from Piatosa et al^{E6} (for lymphocytes, B cells, and B-cell subpopulations), the 10 to 90th percentile and median adopted from Shearer et al^{E7} (for T and natural killer [NK] cells, memory and activated CD4/8⁺ T-cell subpopulations), and the mean and 90% tolerance interval adopted from Schatorjé et al^{E8} (for major T-cell populations and most CD4/8⁺ T-cell subpopulations). Note that gating strategies for cell populations may differ between cited reports and our report.

Additional notes with regard to the analysis of panels shown in Fig 2: A, Absolute numbers of lymphocytes (CD45⁺ and scatter characteristics) and B (CD45⁺CD19⁺), T (CD45⁺CD3⁺), and NK (CD45⁺CD16⁺CD56⁺) cells. B, Relative lymphocyte and B, T, and NK-cell values as indicated by the

percentage of total CD45⁺ leukocytes (lymphocytes) or CD45⁺ lymphocytes (B, T, and NK cells). C, Relative numbers for B-cell subpopulations expressed as a percentage of total CD19⁺ B cells: transitional B cells (CD27⁺IgD⁺IgM⁺CD24⁺CD38⁺); naive B cells (CD27⁺IgD⁺IgM⁺); innate effector/marginal zone B cells (CD27⁺IgD⁺IgM⁺); switched memory B cells (CD27⁺IgD⁺IgM⁺); CD27-negative memory B cells (CD27⁺IgD⁺IgM⁺); plasmablasts (CD27⁺CD38⁺CD24⁺); CD21low CD38low activated B cells (CD21^{lo}CD38^{lo}). D, Relative frequencies of major T-cell subsets: TCR-g/d positive cells (CD45⁺TCRg/d⁺), TCR-g/d negative cells (CD45⁺TCRg/d⁻), CD4⁺T cells (TCRg/d-CD4⁺), CD8⁺ T cells (TCRg/d-CD8⁺), CD4⁺CD8⁺ double-positive T cells (TCRg/d-CD4⁺CD8⁺), and CD4⁻CD8⁻ double-negative T cells (TCRg/d-CD4⁻CD8⁻). Relative cell counts for TCRg-d-positive and TCRg-d-negative T cells indicate the percentage of total CD45⁺ lymphocytes. Relative cell counts for CD4⁺, CD8⁺, double-positive, and double-negative T cells depict the percentage of CD3⁺TCRg-d⁺ T cells. E, Relative frequencies of CD4⁺ T-cell subpopulations: Naive T cells (CD45RA⁺CD27⁺), terminally differentiated T cells (term. diff.; CD45RA⁺CD27⁻), central memory T cells (T_{CM}; CD45RA⁻CD27⁺), effector memory T cells (T_{EM}; CD45RA⁻CD27⁻), recent thymic emigrants (CD45RO⁻CD31⁺CD62L⁺HLA⁻DR⁻), memory T cells (CD45RO⁺), and activated T cells (HLA⁻DR⁺). Relative cell counts for CD4⁺ naive, term. diff., T_{CM}, and T_{EM} T cells depict the percentage of total CD4⁺ lymphocytes. Relative cell counts for CD4⁺ memory and activated T cells depict the percentage of CD3⁺ T cells. F, Relative frequencies of CD8⁺ T-cell subpopulations: Naive T cells (CD45RO⁻CD27⁺CCR7⁺), term. diff. T cells (CD45RO⁻CD27⁺CCR7⁻), T_{CM} (CD45RO⁺CD27⁺CCR7⁺), T_{EM} (CD45RO⁺CD27⁻CCR7⁻), memory T cells (CD45RO⁺), and activated T cells (HLA-DR⁺). Relative cell counts for naive, term. diff., T_{CM}, and T_{EM} T cells depict the percentage of total CD8⁺ lymphocytes. Relative cell counts for memory and activated T cells depict the percentage of CD3⁺ T cells.

REFERENCES

- E1. Lunter G, Goodson M. Stampy: a statistical algorithm for sensitive and fast mapping of Illumina sequence reads. *Genome Res* 2011;21:936-9.
- E2. Rimmer A, Phan H, Mathieson I, Iqbal Z, Twigg SRF, Wilkie AOM, et al. Integrating mapping-, assembly- and haplotype-based approaches for calling variants in clinical sequencing applications. *Nat Genet* 2014;46:912-8.
- E3. Available at: www.evs.gs.washington.edu/EVS/.
- E4. Wallis Y, Payne S, McNulty C, Bodmer D, Sistermans E, Robertson K, et al. Practice Guidelines for the Evaluation of Pathogenicity and the Reporting of Sequence Variants in Clinical Molecular Genetics. Available at: <http://www.acgs.uk.com/committees/quality-committee/best-practice-guidelines/>.
- E5. Martin E, Palmic N, Sanquer S, Lenoir C, Hauck F, Mongellaz C, et al. CTP synthase 1 deficiency in humans reveals its central role in lymphocyte proliferation. *Nature* 2014;510:288-92.
- E6. Piatosa B, Wolska-Kuśnierz B, Pac M, Siewiera K, Gałkowska E, Bernatowska E. B cell subsets in healthy children: reference values for evaluation of B cell maturation process in peripheral blood. *Cytometry B Clin Cytom* 2010;78B:372-81.
- E7. Shearer WT, Rosenblatt HM, Gelman RS, Oymopito R, Plaeger S, Stiehm ER, et al. Lymphocyte subsets in healthy children from birth through 18 years of age: the pediatric AIDS clinical trials group P1009 study. *J Allergy Clin Immunol* 2003;112:973-80.
- E8. Schatorjé EJH, Gemen EFA, Driessen GJA, Leuvenink J, van Hout RWNM, de Vries E. Paediatric reference values for the peripheral T cell compartment. *Scand J Immunol* 2012;75:436-44.

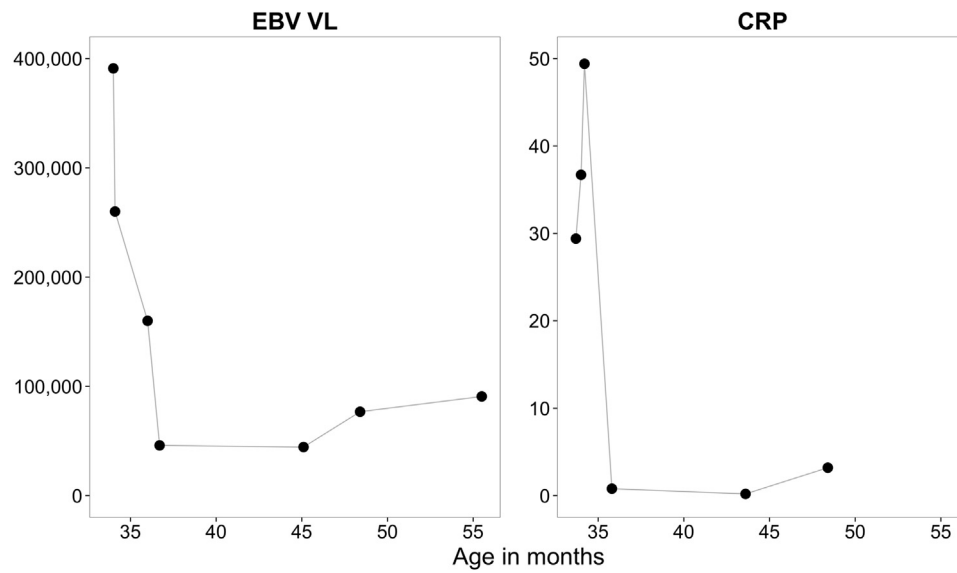


FIG E1. Kinetics of EBV viral load (VL [copies/mL]) and CRP (mg/L) of patient Pat_1.1 during and after the acute EBV infection at around age 34 months.

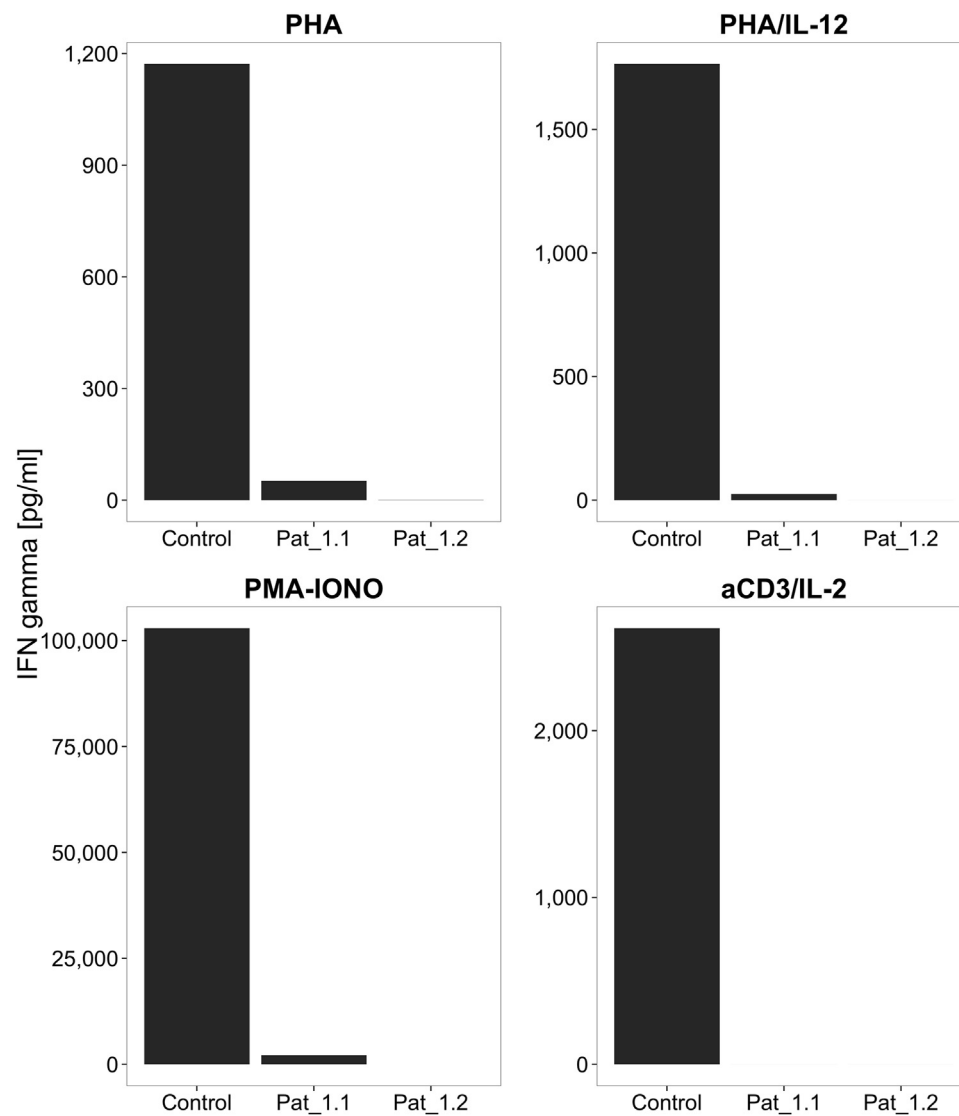


FIG E2. Cytokine studies on both patients (boy, Pat_1.1, and girl, Pat_1.2) and a control. Stimulating agents are shown above each bar graph, and bars show IFN- γ responses to stimulation as bars for both patients in comparison with a healthy control. *IONO*, Ionomycin; *PMA*, phorbol 12-myristate 13-acetate.

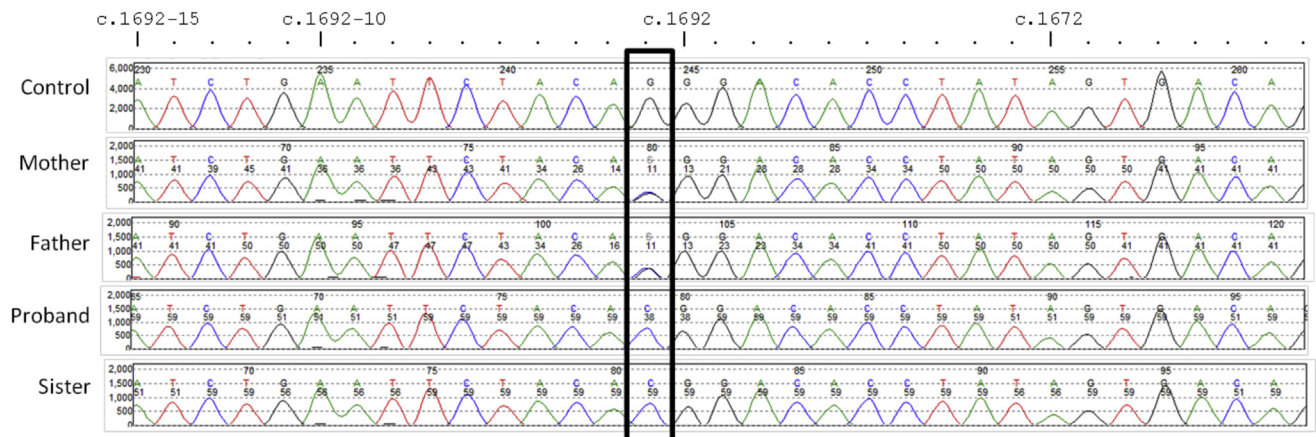


FIG E3. *CTPS1* sequence electropherograms for the 4 members of the kindred with the c.1692-1G > C variant (outlined by the *black box*).

TABLE E1. Results of immunologic investigations performed in the 2 siblings

Patient	P1.1 (male)	P1.2 (female)
Age at evaluation (mo)	42	9
Cell subsets (cells/mm ³)		
ANC (1.5-8.0)	5.15	2.4
Lymphocytes	2.23 (1.8-5.4)	3.11 (2.6-10.4)
CD3 ⁺ (normal)	1.81 (1.2-3.4)	1.99 (1.6-6.7)
CD4 ⁺ (normal)	1.1 (0.8-2.1)	1.45 (1.0-4.6)
CD8 ⁺ (normal)	0.62 (0.35-1.7)	0.5 (0.4-2.1)
CD19 ⁺ (normal)	0.25 (0.1-0.5)	0.89 (0.6-2.7)
CD56 ⁺ (normal)	0.15 (0.1-1.0)	0.2 (0.2-1.2)
T-cell proliferation by CFSE (using PHA)	Normal	ND
Serum immunoglobulins		
IgA (normal) (g/L)	1.01 (0.4-2.0)	0.72 (0.2-0.7)
IgG (normal) (g/L)	5.34 (4.9-13.0)	5.58 (3.0-10.9)
IgM (normal) (g/L)	0.62 (0.4-2.5)	0.44 (0.4-2.0)
IgE (normal) (kU/L)	6.49 (5-63)	ND

Values in boldface correspond to values outside normal age-matched ranges that are indicated in parentheses.

ANC, Absolute neutrophil count; CFSE, carboxyfluorescein succinimidyl ester;

ND, not done.

TABLE E2. List of targeted panel of 237 immune-related genes

<i>ACP5</i>	<i>CD8A</i>	<i>IL10</i>	<i>NHP2</i>	<i>SPINK5</i>
<i>ACTB</i>	<i>CEBPE</i>	<i>IL10RA</i>	<i>NKX2-5</i>	<i>STAT1</i>
<i>ADA</i>	<i>CFB</i>	<i>IL10RB</i>	<i>NLRP12</i>	<i>STAT2</i>
<i>ADAM17</i>	<i>CFD</i>	<i>IL12 B</i>	<i>NLRP3</i>	<i>STAT3</i>
<i>ADAR</i>	<i>CFH</i>	<i>IL12RB1</i>	<i>NOD2</i>	<i>STAT5B</i>
<i>AICDA</i>	<i>CFHR1</i>	<i>IL17F</i>	<i>NOP10</i>	<i>STIM1</i>
<i>AIRE</i>	<i>CFHR2</i>	<i>IL17RA</i>	<i>NRAS</i>	<i>STK4</i>
<i>AK2</i>	<i>CFHR3</i>	<i>IL1RN</i>	<i>ORAI1</i>	<i>STX11</i>
<i>AP3B1</i>	<i>CFHR4</i>	<i>IL21R</i>	<i>PIGA</i>	<i>STXBP2</i>
<i>APOL1</i>	<i>CFHR5</i>	<i>IL2RA</i>	<i>PIK3CD</i>	<i>TAP1</i>
<i>ATM</i>	<i>CFI</i>	<i>IL2RG</i>	<i>PIK3R1</i>	<i>TAP2</i>
<i>BLM</i>	<i>CFP</i>	<i>IL36RN</i>	<i>PLCG2</i>	<i>TAPBP</i>
<i>BLNK</i>	<i>CHD7</i>	<i>IL7R</i>	<i>PMS2</i>	<i>TAZ</i>
<i>BLOCL1S6</i>	<i>CIITA</i>	<i>IRAK4</i>	<i>PNP</i>	<i>TBK1</i>
<i>BTK</i>	<i>COLEC11</i>	<i>IRF8</i>	<i>POLE</i>	<i>TBX1</i>
<i>C1QA</i>	<i>CORO1A</i>	<i>ISG15</i>	<i>PRF1</i>	<i>TCF3</i>
<i>C1QB</i>	<i>CR2</i>	<i>ITCH</i>	<i>PRKCD</i>	<i>TCN2</i>
<i>C1QC</i>	<i>CSF2RA</i>	<i>ITGB2</i>	<i>PRKDC</i>	<i>TERT</i>
<i>C1R</i>	<i>CTPS1</i>	<i>ITK</i>	<i>PSMB8</i>	<i>THBD</i>
<i>C1S</i>	<i>CTSC</i>	<i>JAK3</i>	<i>PSTPIP1</i>	<i>TICAM1</i>
<i>C2</i>	<i>CXCR4</i>	<i>KMT2D</i>	<i>PTPRC</i>	<i>TINF2</i>
<i>C3</i>	<i>CYBA</i>	<i>KRAS</i>	<i>RAB27A</i>	<i>TLR3</i>
<i>C4A</i>	<i>CYBB</i>	<i>LAMTOR2</i>	<i>RAC2</i>	<i>TMC6</i>
<i>C4B</i>	<i>DCLRE1C</i>	<i>LCK</i>	<i>RAG1</i>	<i>TMC8</i>
<i>C5</i>	<i>DKC1</i>	<i>LIG4</i>	<i>RAG2</i>	<i>TNFRSF13B</i>
<i>C6</i>	<i>DNMT3B</i>	<i>LPIN2</i>	<i>RBCK1</i>	<i>TNFRSF13C</i>
<i>C7</i>	<i>DOCK8</i>	<i>LRBA</i>	<i>RFX5</i>	<i>TNFRSF1A</i>
<i>C8A</i>	<i>ELANE</i>	<i>LYST</i>	<i>RFXANK</i>	<i>TNFRSF4</i>
<i>C8B</i>	<i>FADD</i>	<i>MAGT1</i>	<i>RFXAP</i>	<i>TNFSF12</i>
<i>C9</i>	<i>FAS</i>	<i>MALT1</i>	<i>RHOH</i>	<i>TRAF3</i>
<i>CARD11</i>	<i>FASLG</i>	<i>MASP1</i>	<i>RNASEH2A</i>	<i>TRAF3IP2</i>
<i>CARD14</i>	<i>FCN3</i>	<i>MASP2</i>	<i>RNASEH2B</i>	<i>TREX1</i>
<i>CARD9</i>	<i>FERMT3</i>	<i>MBL2</i>	<i>RNASEH2C</i>	<i>TTC7A</i>
<i>CASP10</i>	<i>FOXP1</i>	<i>MCM4</i>	<i>RNF168</i>	<i>TYK2</i>
<i>CASP8</i>	<i>FOXP3</i>	<i>MEFV</i>	<i>RPSA</i>	<i>UNC119</i>
<i>CD19</i>	<i>FPR1</i>	<i>MRE11A</i>	<i>RTEL1</i>	<i>UNC13D</i>
<i>CD247</i>	<i>G6PC3</i>	<i>MS4A1</i>	<i>SAMHD1</i>	<i>UNC93B1</i>
<i>CD27</i>	<i>G6PD</i>	<i>MSH5</i>	<i>SBDS</i>	<i>UNG</i>
<i>CD3D</i>	<i>GATA2</i>	<i>MTHFD1</i>	<i>SEMA3E</i>	<i>USB1</i>
<i>CD3E</i>	<i>GFI1</i>	<i>MVK</i>	<i>SERPING1</i>	<i>VPS13B</i>
<i>CD3G</i>	<i>HAX1</i>	<i>MYD88</i>	<i>SH2D1A</i>	<i>VPS45</i>
<i>CD40</i>	<i>ICOS</i>	<i>NBN</i>	<i>SH3BP2</i>	<i>WAS</i>
<i>CD40LG</i>	<i>IFNGR1</i>	<i>NCF1</i>	<i>SLC29A3</i>	<i>WIPF1</i>
<i>CD46</i>	<i>IFNGR2</i>	<i>NCF2</i>	<i>SLC35C1</i>	<i>XIAP</i>
<i>CD59</i>	<i>IGLL1</i>	<i>NCF4</i>	<i>SLC37A4</i>	<i>ZAP70</i>
<i>CD79A</i>	<i>IKBKB</i>	<i>NFKB2</i>	<i>SLC46A1</i>	<i>ZBTB24</i>
<i>CD79B</i>	<i>IKBKG</i>	<i>NFKBIA</i>	<i>SMARCAL1</i>	
<i>CD81</i>	<i>IKZF1</i>	<i>NHEJ1</i>	<i>SP110</i>	